

Omni-directional person tracking on a flying robot using occlusion-robust ultra-wideband signals

Tobias Nägeli^{1†}, Benjamin Hepp^{1†}, Otmar Hilliges¹

Abstract—We present a tracking system based on ultra-wideband (UWB) radio transceivers mounted on a robot and a target. In comparison to typical UWB localization systems with fixed UWB transceivers in the environment we only require instrumentation of the target with a single UWB transceiver. Our system works in GPS-denied environments and does not suffer from long-term drift and limited fields of view.

This paper reports the localization algorithm and implementation details. Additionally, we demonstrate a quantitative evaluation of the accuracy (10cm average position error for a square with side-length of 4m) and application scenarios with a quadrotor flying in close proximity to a person and handling occlusion of the target.

I. INTRODUCTION

With the increasing mainstream adoption of robotics, operating in close vicinity to humans is becoming an important area of robotics research. Applications range from surveillance to search and rescue and even entertainment scenarios, where small wheeled, flying or swimming robots operate in parallel or cooperatively with one or several human operators. For such robotic-human tandems to operate safely and successfully the robot needs to be able to robustly and accurately locate the human. For example, micro-aerial vehicles (MAVs) equipped with appropriate target localization technology, enable following and close-proximity aerial videography, simple waypoint coverage for surveillance in GPS-denied areas, automatic human following for inspection work or basic tasks such as landing at a charging station. One key challenge in many application scenarios is mobility – rendering the use of infrastructure based localization technologies impractical or even entirely infeasible.

Despite its importance, few technologies are available that could localize objects relative to a robot without any instrumentation of the environment. This is in particular true for small and agile robots that often can not accommodate heavy and power hungry compute hardware. Approaches based on cameras and visual markers may not be acceptable for users due to aesthetic aspects. Robust non-marker based visual tracking is still an open research problem. Visual trackers can suffer from limited fields of view and occlusion by other objects. Existing real-time tracking solutions [1], [2] need to deal with long-term drift and re-detection problems. Tracking in low-light conditions is another challenging issue. While the commercial sector uses GPS for person tracking [3], [4], the attainable accuracy is limited (especially in urban

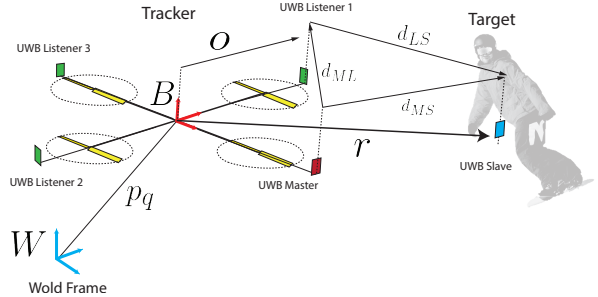


Fig. 1. **Illustration of multi unit ranging**

Shown is a quadrotor with 4 UWB units (*master* in red and *listeners* in green) and a target with a single UWB unit (*slave* in blue).

environments) and reliance on GPS restricts applicability to outdoor use.

To address this problem we propose a mobile and lightweight tracking system based on ultra-wideband (UWB) radio [6], [5], [7]. In contrast to existing work our approach operates in an *inside-out* fashion. That is we mount a small number of receivers onto a robot and track targets outside of the spanned convex hull. This approach is fundamentally different to related UWB-based MAV localization work [8], relying on UWB tags placed at known locations in the environment. Our proposed method operates with a much smaller baseline and does not require any instrumentation of the environment: in addition to the robot mounted transceivers a single tag on the target is sufficient.

To track a target outside of the convex hull we perform trilateration with time-of-arrival (TOA) measurements. This is less sensitive to measurement errors compared to multilateration with time-difference-of-arrival measurements, especially in our *inside-out* use case with a small baseline between UWB units [9]. A novel active-passive ranging algorithm addresses issues with conventional ranging schemes, in which the measurement rate inversely depends on the number of UWB units. Our scheme achieves measurement rates independent of the number of tags and hence is as fast as conventional ranging schemes with a single tag. In comparison to [8] this allows us to circumvent the problem of synchronizing clocks of the target and the tracker units.

In this paper we detail our algorithm and implementation and empirically demonstrate its efficiency and accuracy. In a typical usage scenario with a target moving along a square of 4 meters our approach achieves an average position accuracy of less than 10 cm, where the tracker is

¹Advanced Interactive Technologies Lab, Department of Computer Science, ETH Zurich, 8092 Zurich, Switzerland
bhepp|naegelit|otmar.hilliges@inf.ethz.ch

[†]These authors contributed equally to this work.

located in the center. Furthermore, we show the usefulness of this tracking approach with a quadrotor that flies around or follows a target object without requiring line-of-sight. Finally, we demonstrate how our approach could be useful in mixed-initiative scenarios by realizing an implicit collision avoidance scheme, where the robot flies along the mapped path of a human, rather than following via the shortest path.

In particular, we contribute a novel vision-less, omnidirectional and lightweight tracking system for use on small, agile robots such as quadrotors. The system is robust to occlusions in unstructured, man-made environments. Furthermore, we propose an active-passive ranging algorithm for *multiple* UWB units, achieving a measurement rate equal to a conventional two-way ranging for a *single* UWB unit. The time required for ranging is independent of the number of UWB units in our approach. Finally, we demonstrate the utility of the method in a path-following scheme with implicit obstacle avoidance by mapping the targets trajectory.

II. SYSTEM OVERVIEW

We propose a mobile tracking system based on trilateration with readily available Ultra-wideband (UWB) radio transceivers mounted on a quadrotor as can be see in Fig. 1. The system consists of a tracker made up of multiple UWB units arranged in a rigid configuration and a target made up of a single UWB unit. Experiments were performed with a tracker consisting of 4 UWB units, however our approach is general and scalable to more units.

We use a novel active-passive ranging algorithm to measure time-of-flight (TOF) from the tracker units to the target unit. A per-unit calibration of the UWB transceivers, described in Sec. IV-A, is used to convert TOF measurements to metric distances. An iterated Extended Kalman filter (IEKF) tracks the 3D position of the target. Finally, the mapped position is used to follow a person with a quadrotor. Our system consists of the following components:

a) Active-passive ranging algorithm: To localize a target we require multiple range measurements. We propose a mixed active-passive ranging algorithm to obtain time-of-flight measurements from multiple UWB units with higher rate than possible with conventional symmetric two-way ranging.

b) Measurement model: The ranging algorithm provides us with time-of-flight measurements. These measurements are subject to noise and to multi-path effects. We model the line-of-sight measurements with an affine mapping and handle multi-path effects using statistical outlier detection.

c) Target Estimation: We localize the target with respect to the quadrotor by trilateration [6]. To deal with the above noisy range measurements. We propose an Iterated Extended Kalman Filter (IEKF) to handle the highly nonlinear measurement model and to obtain a robust estimate.

d) Target Following: To follow the user in a cluttered environment we need to avoid obstacles. Therefore we propose an implicit collision avoidance by mapping and following the users path.

A. Notation and Coordinate Frames

Rotation matrices performing rotations from frame I to frame B are denoted by $\mathbf{R}_{BI} \in SO(3)$, where $SO(3)$ is the special Lie group of all rotations. Note that the columns of \mathbf{R}_{WC} are the basis vectors of coordinate frame C as seen in coordinate frame W . Expected or estimated values of a random variable x are indicated with a hat $\mathbb{E}[x] = \hat{x}$. Positions in the world frame are denoted as $\mathbf{p}_{(\cdot)}$ and relative distances are denoted as $\mathbf{r}_{(\cdot)}$ or $\mathbf{d}_{(\cdot)}$. Timestamps for a unit U and a message m are denoted as τ_U^m . Time-of-flight from unit U to unit W is written as ξ_{UW} and the distance as d_{UW}

III. METHOD

In this section we give an in-detail description of the above mentioned components.

A. Active-passive ranging algorithm

To track a dynamic object with multilateration we require accurate distance measurements with a high rate. We use UWB radio transceivers in a rigid configuration on the tracker to measure time-of-flight to a target UWB unit. From the time-of-flight (TOF) we can easily compute the distance by multiplication with the speed of light.

TOF is commonly measured with two-way ranging where a message is sent from a *master* to a *slave* and the *slave* replies within a specified delay known to the *master*. By subtracting the known delay from the total measured round-trip-time the *master* can estimate the TOF. As the delay is typically orders of magnitude larger than the TOF, a difference in clock frequency (clock skew) between *master* and *slave* has a profound effect on the estimated TOF. This can be mitigated by performing symmetric two-way ranging where a two-way ranging is performed between *master* and *slave* and between *slave* and *master*. The *slave* then reports its measurements to the *master*. We refer the reader to [7] for more details.

For our use-case we identify two problems of TOF measurements with UWB and symmetric two-way ranging. First, when computing ranges from TOF measurements the signal is assumed to have taken a direct line-of-sight (LOS) path. However, due to ambiguities in detection of the first path, especially in environments with occlusions, the TOF measurements can result from a non-line-of-sight (NLOS) path of the signal and thus lead to a wrong TOF and distance estimate. The second problem concerns the measurement rate of a tracker with N units. Performing symmetric two-way ranging results in an overall measurement rate of R/N , where R is the measurement rate for a single UWB unit. This is undesirable for tracking of moving objects.

To be robust towards multipath-environments and occluded LOS paths between tracker and target we employ a hardware protocol configuration that results in more reliable first-path detection [10], [11] (see IV-C). On the downside this configuration results in long message transmission times and inevitably leads to lower measurement rates. To increase the overall measurement rate we **extend the symmetric two-way ranging to an active-passive scheme**. We perform

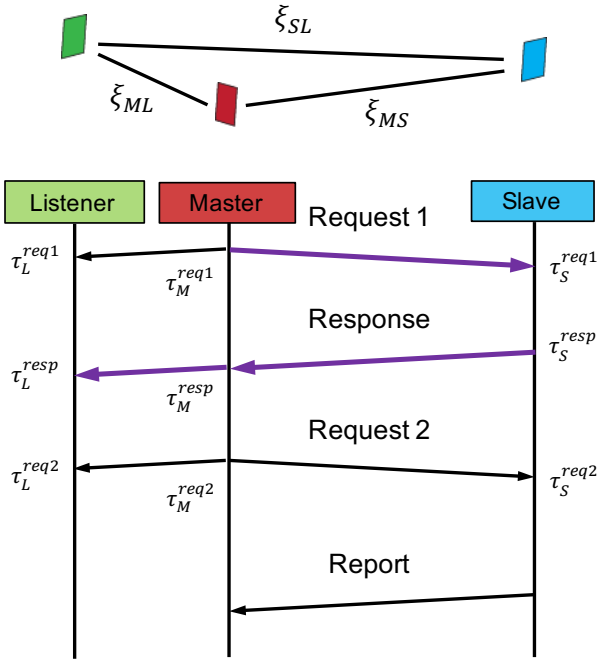


Fig. 2. Illustration of multi unit ranging

Top: Shown are time-of-flights between *master*, *slave* and *listener* units. **Bottom:** Depicted is our ranging protocol. The *master* and the *slave* perform standard symmetric two way ranging. Simultaneously the *listener* receives messages from both the *master* and the *slave*. The timestamps of transmission and reception are recorded for all units measured with their local clock. The violet path shows the trip-time from the *master* over the *slave* to the *listener*. This is used in Algorithm 1 to compute the time-of-flight from *listener* to *slave*. Importantly, the *master* and *listener* are connected to the same computer. Otherwise a report with timestamp measurements of the *listener* would have to be send to the *master* as well.

ranging with multiple UWB units with the same rate as single range measurements, i.e. **for N units on the tracker we achieve a speedup by a factor of N** compared to conventional symmetric two-way ranging. Importantly, we do not require hardware synchronization of the UWB units and thus our approach is generally applicable.

For sake of brevity we describe the case of one *master* and one *listener*. The extension to more *listeners* is straightforward. The *master* unit on the tracker is active and performs symmetric two-way ranging with a *slave* unit on the target [7]. The *listener* unit on the tracker is passive and only receives messages from the *master* and the *slave*. The measurement of each unit consists of the transmission and reception timestamps according to the local clock as depicted in Fig. 2. Each timestamp is denoted as τ_U^{msg} , where U is the unit (M for master, S for slave and L for listener) and msg is the message type ($req1$, $req2$ for request 1, 2 and $resp$ for the response).

The ranging computation is described in Algorithm 1. We first compute the TOF from master to slave using the symmetric two-way ranging algorithm. Next we estimate the response delay δ_S of the *slave* and the total trip time θ from *master* over *slave* to *listener* (see violet path in Fig. 2). The trip time θ is computed using the local timestamps

Algorithm 1 Active-passive Ranging

Require: Distance d_{ML} between *master* and *listeners*. Timestamp measurements τ as depicted in Fig. 2.

Symmetric two-way ranging [7]:

- 1: $t_1 = 2\tau_M^{resp} - \tau_M^{req1} - \tau_M^{req2}$
- 2: $t_2 = -2\tau_S^{resp} + \tau_S^{req1} + \tau_S^{req2}$
- 3: $\xi_{MS} = (t_1 + t_2)/4$

Time-of-flight computation from listener to slave:

- 4: $\delta_S = \tau_M^{resp} - \tau_M^{req1} - 2\xi_{MS}$
- 5: $\Delta\tau_M = \tau_M^{req2} - \tau_M^{req1}$
- 6: $\Delta\tau_L = \tau_L^{req2} - \tau_L^{req1}$
- 7: $\rho_L = \frac{1/\Delta\tau_L - 1/\Delta\tau_M}{1/\Delta\tau_M}$
- 8: $\xi_{ML} = d_{ML}/c$
- 9: $\theta = (\tau_L^{resp} - \tau_L^{req1})(1 + \rho_L) + \xi_{ML}$
- 10: $\xi_{LS} = \theta - \delta_S - \xi_{MS}$

of the *listener* corrected by the clock skew ρ_L and adding the known TOF ξ_{ML} from *master* to *listener*. Finally, we compute the TOF ξ_{LS} from *listener* to *slave* by subtracting the response delay δ_S and the TOF ξ_{MS} from the trip time θ .

In summary, the algorithm provides us with TOF measurements from *master* to *slave* and *listener* to *slave* with the same measurement rate as for a single UWB unit using symmetric two-way ranging. Thus, for our setup with 4 UWB units on the tracker we achieve an effective speedup factor of 4. These measurements are the basis for our tracking method.

B. Measurement Model

We model the UWB module as a ranging device which provides us time-of-flight ξ_{MS} measurements between two sensors e.g. the *master* and the *slave* device. According to [10] we use a first order model to compute metric distances. Therefore the full sensor model is given by

$$d_{MS} = p_0 + p_1\xi_{MS} \quad \text{with} \quad d_{MS} = \|d_{MS}\| \in \mathbb{R}^1 \quad (1)$$

where $d_{MS} \in \mathbb{R}^3$ is the distance vector between the two sensors e.g. *master* and *slave*. The antenna delay [10], speed-of-light and other calibration parameters are covered by this model. The estimation of model parameter p_0 and p_1 is explained in IV-A. The measurement z_{MS} of the distance d_{MS} is corrupted with two sources of noise, a zero-mean gaussian additive noise η with a variance σ_s and a non-linear multiplicative multipath noise λ . Therefore we can extend the sensor model in (1) with these two noise-terms:

$$z_{MS} = \lambda d_{MS} + \eta \quad \text{with} \quad \eta \sim \mathcal{N}(0, \sigma_s), \quad \lambda \geq 1 \quad (2)$$

As we can see in Fig. 1 the UWB sensors are arranged rigidly on the Quadrotor where the distance between two sensors d_{ML} is much smaller than the distance between the target and the quadrotor r . We can conclude from geometrical and theoretical derivations that the expected accuracy of the estimated relative position between the quadrotor and the

target increases with radial distance. The multiplicative noise λ is 1 if we measure the direct line-of-sight distance and $\lambda > 1$ if the module measures an indirect path. We explain in Sec. III-C.2 how we deal with this.

C. Target Estimation

In the next section we describe how we compute from the individual raw distance measurements d_i the relative position \mathbf{r}_t between the target and the quadrotor. A straightforward approach would be to use all 4 measurements and perform gauss-newton to compute the relative target position \mathbf{r} . However, due to special noise characteristics, which will be explained in Sec. III-C.2, we use an Iterated EKF (IEKF) which can deal better with the noise characteristics. The direct comparison can be seen in Fig. 6. We first start with the target model description which is followed by the estimator explanation.

1) *Modeling*: Due to the absence of any feed forward information about the target movement we use a constant velocity model in the world frame $\dot{\mathbf{r}}_t = \mathbf{v}$ with $\mathbf{v} \sim \mathcal{N}(0, \sigma_t)$. Where we can interpret the standard-deviation $\sqrt{\sigma_t}$ as the maximal acceleration of the target. We can write the position \mathbf{p}_t of the person in the world frame as the superposition $\mathbf{p}_t = \mathbf{p}_q + \mathbf{r}$ of the quadrotor position \mathbf{p}_q and the relative distance \mathbf{r} . We assume that the position of the quadrotor \mathbf{p}_q is given (e.g. by GPS or Visual Inertial Odometry [12]) and therefore the position of the quadrotor as well as its velocity is assumed to be known.

We only model the relative position \mathbf{r} and motion $\dot{\mathbf{r}}$ between the target and the quadrotor and will compute the absolute target position \mathbf{p}_t into the world frame in a second step. The relative state is given as $\mathbf{x} = [\mathbf{r}_t, \mathbf{v}_t]^T \in \mathbb{R}^6$.

Discretization and first order Euler integration of the mass-point model given above leads us to the following state-space representation:

$$\mathbf{x}_{k+1} = F\mathbf{x}_k \quad \text{with} \quad F := I_3 \otimes \begin{bmatrix} 1 & dt \\ 0 & 1 \end{bmatrix} \quad (3)$$

with I_3 the 3×3 identity matrix and \otimes the Kronecker product.

2) *Iterated EKF*: As described above we use an Iterated EKF estimator. The prediction step using the linear model given in (3) is straightforward.

For the measurement model we start with the sensor equation given in (1). The vector d_{MS} is distance between the target and the quadrotor, r , and the offset o between the UWB sensor and the quadrotors center of mass. The estimated time-of-flight h_ξ between the sensor and the target is given by inverting the sensor model equation (1):

$$h_\xi(\mathbf{x}) = \frac{\|\mathbf{r} - \mathbf{o}\| - p_0}{p_1} \in \mathbb{R}^1 \quad (4)$$

The Jacobian of the measurement observation model (4), denoted as $H(\mathbf{x})$, is computed in every time-step by linearizing the observation model for all UWB sensors $h_{\xi_i}(\mathbf{x})$. For

the four sensors mounted on the quadrotor we get:

$$H = \left[\frac{\partial h_{\xi_1}(\hat{\mathbf{x}})^T}{\partial \hat{\mathbf{x}}}, \quad \dots, \quad \frac{\partial h_{\xi_4}(\hat{\mathbf{x}})^T}{\partial \hat{\mathbf{x}}} \right]^T \in \mathbb{R}^{4 \times 6}$$

$$\frac{\partial h_{\xi_i}(\mathbf{x})}{\partial \mathbf{x}} = \left[\frac{1}{2p_{1,i}\|\mathbf{r}-\mathbf{o}_i\|} \mathbf{r}^T, \quad 0, \quad 0, \quad 0 \right] \in \mathbb{R}^{1 \times 6}$$

Due to the non-linear measurement equation we use an Iterated EKF. The prediction and update equations are according to [13]. To be robust to multi-path effects and other measurement outliers we perform a χ^2 -test based on the Mahalanobis distance of the residuals. Outliers are detected according to:

$$\mathbf{z}_i^2 = (\mathbf{z} - h_\xi(\mathbf{x}))^T \mathbf{S}_i^{-1} (\mathbf{z} - h_\xi(\mathbf{x})) \geq \chi_{thresh}^2 \quad ,$$

where χ_{thresh}^2 is equal to the 0.9 probability quantile of the χ^2 distribution.

D. Target Following

The absolute, which is assumed to be known (e.g. estimated with GPS, VIO [12] or Vicon), quadrotor position \mathbf{p}_q is controlled according to [14]. Because the relative position estimates \mathbf{r} between quadrotor and target are noisy we do not directly use \mathbf{r} as the setpoint for the position controller. Rather we introduce a trajectory and controller on top. The absolute position \mathbf{p}_t of the target is given by $\mathbf{p}_t = \mathbf{p}_q + \mathbf{R}_{BI}\mathbf{r}$. The trajectory controller drives the reference \mathbf{s} of the position controller towards the desired reference $\bar{\mathbf{s}}$:

$$\mathbf{s}_{k+1} = \mathbf{s}_k + K_p(\bar{\mathbf{s}} - \mathbf{s}_k)$$

The desired reference $\bar{\mathbf{s}}$ is provided by a trajectory generator. This creates new reference keypoints whenever the actual target position \mathbf{p}_t is more than a certain distance threshold γ_t away from the latest stored reference waypoint (see Fig. 4).

$$\mathbf{s}_k = \mathbf{p}_t \quad \text{if} \quad \|\mathbf{s}_{k-1} - \mathbf{p}_t\| \geq \gamma_t$$

The trajectory controller sets the current position setpoint to m step delayed target position \mathbf{s}_{k-m} serves as the quadrotor set-point. The set-point controller is implemented as a P controller:

$$\mathbf{s}_{k+1} = \mathbf{s}_{k-m} + K_p(\mathbf{s}_{k-m} - \mathbf{r}_{s,t})$$

for the delayed trajectory following mode. In summary this approach results in a delayed trajectory following mode.

IV. IMPLEMENTATION DETAILS

A. Calibration

We use an affine mapping to convert TOF measurements from the UWB units to ranges. In comparison to a linear mapping The constant offset can compensate antenna delays [10] and other non-modeled effects. To find the affine mapping we perform an offline calibration based on ground-truth data from a motion capture system. Importantly, we calibrate each UWB unit on the tracker independently to accommodate for fabrication uncertainties between units.



Fig. 3. **Quadrotor with UWB units.**

Shown is a custom-built quadrotor based on the open-source PixFalcon and the commercially available Bebop frame. The UWB units are clearly visible at the end of the four carbon poles. The rotor distance is approximately 20 cm.

B. Hardware Setup

The hardware used in all experiments is based on a commercially available Bebop¹ frame. We use a custom setup based on a PixFalcon Autopilot², available as open-source software. An additional Odroid XU4 single-board PC from Hardkernel³ is used for target position estimation and high level quadrotor trajectory control. UWB units are interfaced with a Nucleo-F411RE development board from STMicroelectronics⁴. The UWB units are commercially available DWM1000 modules from DecaWave⁵.

Communication between Nucleo-F411RE and DWM1000 modules is done over an SPI bus. We point out that this communication can be problematic and brittle with long cables and proper isolation is necessary.

C. UWB measurements

The UWB units are compliant with IEEE 802.15.4a which specifies different transmission configurations. To be robust towards multipath-environments and occluded line-of-sight between *master* and *slave* we employ a low data rate of 110 kbps, a long preamble sequence of 1024 symbols and a pulse repetition rate of 16 MHz [10], [11]. With this configuration the air-time of a message with a small payload takes more than 2.5ms. We need to send four messages for a single range measurement, adding up to 10ms and leading to a measurement rate of 100Hz for a single UWB unit. Consequently, the measurement rate with a setup of 4 UWB units on the master and using a conventional ranging method is about $100\text{Hz}/4 = 25\text{Hz}$. Including message payloads and processing time of the ranging algorithm we end up with a rate of approximately 20Hz. With our active-passive scheme we achieve rates of approximately 80Hz because we can perform the range measurement for all units simultaneously without sending individual messages for each unit. The additional processing and communication time with

the DWM1000 modules is negligible. For more information on UWB we refer the reader to [5].

D. Quadrotor

The quadrotor is controlled in a global coordinate frame and localized with a motion capture system, however other localization methods such as GPS or visual odometry could also be used. The UWB units are arranged in a horizontal plane on the quadrotor and therefore we track the position in 2D in the same plane. With a suitable frame an additional UWB unit could be placed out of the horizontal plane.

V. EXPERIMENTAL RESULTS

A. Experiments

We conducted two experiments to evaluate and validate our approach.

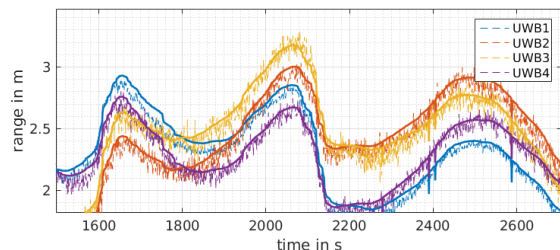


Fig. 5. **Comparison of UWB range measurements and ground truth** Plotted are range measurements from UWB units (dashed) and corresponding ground truth (solid). Measurements of the *master* are plotted in blue.

1) *Experiment 1 (Accuracy)*: We keep the tracker fixed and map a target moving along a square with a side-length of 4m. Ground-truth ranges and poses are measured with a motion-capture system. Fig. 5 shows UWB ranges and corresponding ground-truth. The trajectory of the target is depicted in Fig. 6. Estimation is plotted in blue, ground-truth in red. We achieve an average error of less than 10cm when walking along a square with a side-length of 4meters). Additionally, we show individual trilateration without a filter in red. The trajectory estimated with the filter has a significantly lower average error (10cm vs 22cm).

2) *Experiment 2 (Path mapping and following)*: In this experiment a person walks through an unstructured environment with occlusions and obstacles (see Fig. 4). As described in Sec. III-D the quadrotor maps the estimated target position p_q in the global frame and follows with a delay. The controller gain K_p was kept low to prevent jumping movements of the quadrotor. Despite the complex arrangement of obstacles and occlusions the quadrotor was able to follow the person without collision. We refer to the supplementary video for a better demonstration.

VI. CONCLUSION

In this work we presented a mobile, lightweight tracking system based on UWB radio transceivers mounted on a mobile robot. The system is omni-directional and is robust to obstacles and occlusions between tracker and target.

¹<http://www.parrot.com/de/>

²<http://www.pixfalcon.com/>

³<http://www.hardkernel.com/>

⁴<http://www.st.com/stm32nucleo>

⁵<http://www.decawave.com/>



Fig. 4. **Path mapping and following experiment** Shown is the quadrotor successfully mapping a human holding a target unit using the position estimate from the UWB measurements. The quadrotor follows the mapped path in a delayed fashion. This leads to an implicit collision avoidance. The path is highlighted in red and the mapped reference keypoints \bar{s} in black. The absolute position of the quadrotor is provided by a motion capture system. Note that the mapping is performed through obstacles.

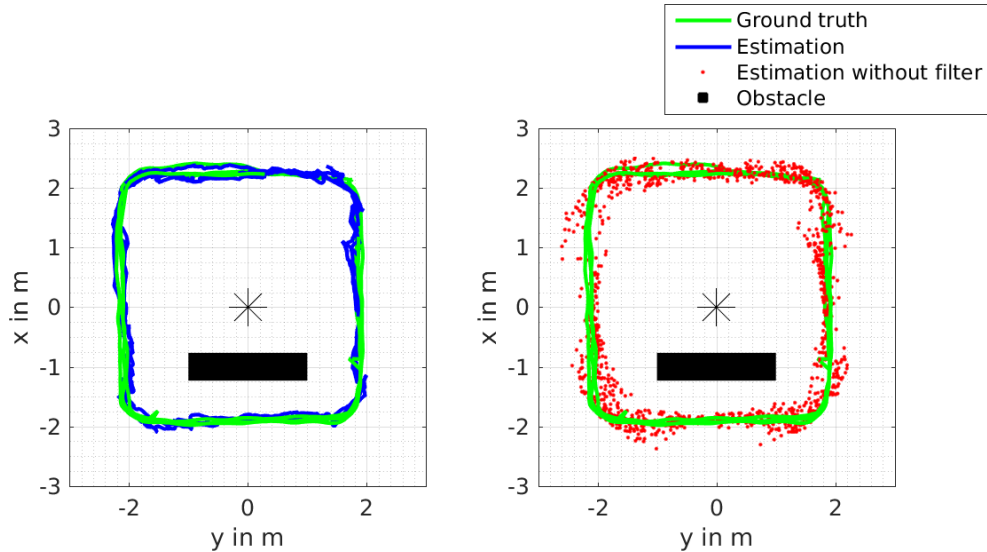


Fig. 6. **Estimated target trajectory and ground truth**

The target was moved along a square around the tracker. Shown on the left is the trajectory (red) estimated by trilateration independently on each measurement. Shown on the right is the trajectory estimated with our Iterated Kalman Filter (IEKF). In both cases the ground truth trajectory is shown in green, the cross shows the location of the tracker and the black rectangle depicts an occluding wall between tracker and target.

Possible future directions include investigation of improving rejection of multi-path measurements, simultaneous tracking of multiple targets and performing quadrotor flight based on only relative position estimates from our tracking system.

REFERENCES

- [1] J. Pestana, J. L. Sanchez-Lopez, S. Saripalli, and P. Campoy, "Computer vision based general object following for gps-denied multirotor unmanned vehicles," in *American Control Conference (ACC), 2014*. IEEE, 2014, pp. 1886–1891.
- [2] H. Lim and S. N. Sinha, "Monocular localization of a moving person onboard a quadrotor mav."
- [3] "airdog," <https://www.airdog.com/>, accessed: 2010-09-30.
- [4] "lily," <https://www.lily.camera/>, accessed: 2010-09-30.
- [5] L. Yang and G. B. Giannakis, "Ultra-wideband communications: an idea whose time has come," *Signal Processing Magazine, IEEE*, vol. 21, no. 6, pp. 26–54, 2004.
- [6] S. Gezici, Z. Tian, G. B. Giannakis, H. Kobayashi, A. F. Molisch, H. V. Poor, and Z. Sahinoglu, "Localization via ultra-wideband radios: a look at positioning aspects for future sensor networks," *Signal Processing Magazine, IEEE*, vol. 22, no. 4, pp. 70–84, 2005.
- [7] M. Yavari and B. G. Nickerson, "Ultra wideband wireless positioning systems," *Dept. Faculty Comput. Sci., Univ. New Brunswick, Fredericton, NB, Canada, Tech. Rep. TR14-230*, 2014.
- [8] A. Ledergerber, M. Hamer, and R. D'Andrea, "A robot self-localization system using one-way ultra-wideband communication," in *Intelligent Robots and Systems (IROS), 2015 IEEE/RSJ International Conference on*. IEEE, 2015, pp. 3131–3137.
- [9] G. Mao and B. Fidan, "Localization algorithms and strategies for wireless sensor networks," pp. 7–13, 2009.
- [10] *DW1000 USER MANUAL - How To Use , Configure and Program the DW1000 UWB*, DecaWave Ltd 2015, 2015.
- [11] *APS006 APPLICATION NOTE - CHANNEL EFFECTS ON COMMUNICATIONS RANGE AND TIME STAMP ACCURACY*, DecaWave Ltd 2015, 2014.
- [12] P. Tanskanen, T. Naegeli, M. Pollefeys, and O. Hilliges, "Semi-direct ekf-based monocular visual-inertial odometry."
- [13] W. F. Denham and S. Pines, "Sequential estimation when measurement function nonlinearity is comparable to measurement error," *AIAA journal*, vol. 4, no. 6, pp. 1071–1076, 1966.
- [14] T. Naegeli, C. C. and A. Domahidi, M. Morari, and O. Hilliges, "Environment-independent formation flight for micro aerial vehicles," in *Proc. of The International Conference on Intelligent Robots and Systems (IROS)*, 2014.